

Renormalized jellium mean-field approximation for binary mixtures of charged colloidsJosé Marcos Falcón-González¹ and Ramón Castañeda-Priego^{1,2,*}¹*División de Ciencias e Ingenierías, Campus León, Universidad de Guanajuato, Loma del Bosque 103, Lomas del Campestre, 37150 León, Guanajuato, Mexico*²*Center for Neutron Science, Chemical Engineering Department, University of Delaware, 150 Academy Street, Newark, Delaware 19716, USA*

(Received 3 November 2010; revised manuscript received 10 February 2011; published 4 April 2011)

In this work the renormalized jellium model of colloidal suspensions, originally proposed by Trizac and Levin [Phys. Rev. E **69**, 031403 (2004)], is extended to study mechanisms of charge renormalization in binary mixtures of charged colloids. We here apply our recent reformulation that introduces the requirement of self-consistency directly into the Poisson-Boltzmann equation, i.e., the background charge is explicitly replaced by the effective one, thus facilitating the whole charge renormalization scheme. We briefly discuss the reformulated model for monodisperse charged suspensions composed of either spheres or rods. In particular, we put emphasis on the effects of the surface charge variation, mixture composition, and particle size on the charge regulation of charge-stabilized colloidal suspensions.

DOI: [10.1103/PhysRevE.83.041401](https://doi.org/10.1103/PhysRevE.83.041401)

PACS number(s): 82.70.Dd, 61.72.Lk

I. INTRODUCTION

During the past few decades charged colloidal suspensions have been the subject of intense research. The origin of such interest resides in the fact that charged colloids are important for either industrial or medical applications and, from a statistical mechanics point of view, represent a unique model system to understand both the phase behavior and the effective interaction potentials in many-body systems [1,2].

Effective interactions appear naturally in the description of colloidal systems because, on the one hand, most of the experimental techniques [3,4] are not able to probe all the components in the system, i.e., solvent molecules and microions, and, on the other hand, the incorporation of all the degrees of freedom in any theoretical framework is an impossible task. Hence, one has to deal with different levels of description that permit us to explain and understand, for instance, the suspension thermodynamics or both static and dynamic correlations between charged colloids, see, e.g., Refs. [1,2] and references therein.

In the simplest level of description, one usually considers the solvent as a dielectric continuum of permittivity ϵ . This description is known as the primitive model and cannot be applied directly to study a real colloidal suspension due to the large difference in size and charge between the colloids and microions. However, it is common to map a charged colloidal suspension onto an asymmetric electrolyte [1,5–12]. This mapping is restricted to moderate charge asymmetries due to the treatment of long-range interactions becoming a time-consuming problem. One way to overcome this situation is to implement many-colloid mean-field computations [13,14]. At this level, the microions are integrated out of the description and the force on any colloid depends on the positions of all other colloids in the system. Technically, this is done by solving the nonlinear Poisson-Boltzmann (PB) equation for each colloidal configuration; the so-called multicentered PB solver is described in detail in Ref. [14]. Unfortunately, this procedure also becomes very demanding, in particular,

at moderate and high particle concentrations. Then, one has to resort to arguments of isotropy and homogeneity of the whole suspension to assume that the microion distribution is symmetric around each charged colloid. Thus, the resulting PB equation is now tractable and provides a good estimation of the system osmotic pressure within the weak coupling regime [15].

Poisson-Boltzmann-based approximations are useful not only to evaluate thermodynamic properties of charged colloidal suspensions but also to account for condensation of counterions onto charged polyelectrolytes [1,2,16–21] or to explain complex transport phenomena in biological systems, such as the nonmonotonic density dependence of the diffusion of DNA fragments [22]. However, alternative frameworks that also describe the condensation effect or charge renormalization have been proposed in recent years. For example, approximations based on integral equations theory that incorporate explicitly solvent details allow us to understand the charge renormalization in nanoparticle dispersions [23–26]. Nevertheless, such approximations cannot be straightforwardly applied to situations in which particles are highly charged or in concentrated suspensions. Therefore, one has to deal with mean-field approaches that are able to explain some of the physical properties in such cases. However, mean-field models also need further approximations at different levels, for instance, in the Hamiltonian [19–21] or directly into the PB equation [27,28], for their solution. Interestingly, even the simplest degree of approximation leads to results that usually agree nicely with either primitive model simulations or experiments [21].

Within the PB mean-field description, the ion-ion correlation is completely neglected and in some models (cell- and jellium-like) the colloid-colloid correlation is introduced *a priori* by assuming a given form for the radial distribution function between colloids. Additionally, the PB description allows us to compute the effective (charge and screening) parameters when a Yukawa-like potential among colloids is explicitly assumed. It is known that this particular potential accurately reproduces the long-distance interaction of two colloids immersed in a salt sea but it should be kept in mind that it usually fails at short distances [29]. Moreover, it has been demonstrated that the force that a colloid feels due to the

*ramoncp@fisica.ugto.mx

interaction with its neighbors cannot be written as a sum of pairs only [15].

Recently, the so-called PB-cell model [28,30] and renormalized jellium (RJ) approximation [27] have been tested against many-body and primitive model calculations to prove their accuracy for determining both the osmotic pressure and the microstructure of colloids immersed in an aqueous environment and in contact with a symmetric (1:1) salt reservoir [15]. Dobnikar *et al.* [15] explicitly showed that both approximations give good results, although the RJ provides higher accuracy for those systems within the fluid phase and far away the (possible) liquid-solid transition. The RJ is an extension of the original jellium work proposed by Beresford-Smith *et al.* [31]; the latter did not include a renormalization of the charge. Due to its simplicity, the RJ model has successfully been incorporated or extended to different situations. For example, to include colloid-colloid correlations [32,33], to incorporate thermodynamic self-consistency to fit experimental data [3], and for systems made up of nonspherical particles [34]. In a recent work, Colla and Levin [35] have extended the RJ model to account for charge renormalization in colloidal suspensions containing trivalent counterions.

In a previous work, we have revisited the RJ model [36]. In such a work, we described its practical reformulation for monodisperse systems; however, its full analysis and implementation to other cases of interest has not been discussed in detail. The aim of this work, then, is to show that the reformulated RJ approximation [36] can be easily extended and adapted to different systems. Particularly, we here review briefly the case of monodisperse suspensions composed of charged spheres or rods. We mainly put emphasis in the case of a binary mixture of charged colloids to account for polydispersity effects in the charge renormalization mechanisms of charged colloids in suspension.

After the Introduction, Sec. II describes briefly the main elements of the RJ approximation originally proposed by Trizac and Levin [27] and its reformulation for the cases of spheres and rods. We compare our results with both the original RJ and the PB-cell models. Section III deals with the extension of the renormalization procedure to the case of a charged binary mixture. Finally, the paper ends with a section of concluding remarks.

II. RENORMALIZED JELLIUM MODEL

A. Main idea

When colloidal particles are immersed in a polar aqueous continuum medium, a dissociation of counterions occurs, which, together with other microions (ions from the salt reservoir) in the solution, creates an inhomogeneous charged cloud around each colloid. Usually, in a simplified one-component model (OCM) the macroion and its ions cloud are considered as a spherical object with an effective charge Z_{eff} , whereas the effective interaction potential between macroions is assumed to be of the Yukawa-like form with effective parameters, namely effective charge and effective Debye screening length, κ^{-1} . Within the OCM the main task is to develop a scheme that provides a simple recipe for the calculation of such effective parameters. Recently, it has been

demonstrated that the so-called renormalized jellium model [27] provides accurate values for the effective parameters and the system thermodynamics of charged colloids in suspension [15].

The system under consideration is composed of N_c colloidal particles immersed in a sea of counterions and in contact with a symmetric (1:1) salt reservoir of concentration $2c_s$, c_s being the density of positive or negative salt ions; the solvent is included through the dielectric constant ϵ . The RJ model assumes that the charge of $N_c - 1$ colloidal particles around a tagged macroion is smeared out in the whole suspension to form a homogeneous background with a charge $Z_{\text{back}}e$, e being the elementary charge. This background charge is enforced to coincide with Z_{eff} of the tagged macroion [27], which possesses a bare charge $Z_{\text{bare}}e$.

The key point in the Trizac and Levin approach [27] is that $Z_{\text{back}} \neq Z_{\text{bare}}$. Within the original RJ approach, the effective charge is a function of both background and bare charges, i.e., $Z_{\text{eff}} = Z_{\text{eff}}(Z_{\text{back}}, Z_{\text{bare}})$, and self-consistency is reached when the relation

$$Z_{\text{back}} = Z_{\text{eff}}(Z_{\text{back}}, Z_{\text{bare}}) \quad (1)$$

is fulfilled. This condition allows to compute numerically the *a priori* unknown background charge [27].

B. Reformulation of the renormalized jellium approximation

1. Charged spherical colloids

As we discussed previously, the RJ model allows us to obtain the effective charge of a monodisperse charged colloidal suspension. This key quantity is directly associated to the system osmotic pressure, the screening parameter, and the effective pair interaction between colloids (when it is explicitly considered at the level of the Yukawa approximation) [15]. Nevertheless, its calculation is not a straightforward task, since it is an explicit function of the system state, i.e., $Z_{\text{eff}} = Z_{\text{eff}}(\eta, Z_{\text{bare}}, c_s)$, where $\eta \equiv \frac{\pi}{6}\sigma^3\rho$ is the volume fraction, with σ and ρ being the particle diameter and number particle density, respectively. This means that the whole iterative protocol described in Ref. [27] must be performed for the specific conditions of each system. This route, of course, becomes tedious and time-demanding from the computational point of view. However, we have shown that the RJ model can be reformulated [36] in order to gain clarity in the way in which the RJ can be straightforwardly applied and easily extended to study the physical properties of more complex charge-stabilized colloidal suspensions.

Within the reformulated model the requirement of self-consistency is introduced from the beginning [36]. This means that the condition

$$Z_{\text{back}} = Z_{\text{eff}}, \quad (2)$$

must be explicitly incorporated into the Poisson-Boltzmann equation [27]. Our main assumption is that there exists a unique Z_{eff} for a given Z_{bare} ; this avoids completely the inclusion of Z_{back} in the whole problem and, thus, facilitates drastically the renormalization scheme [36]. Additionally, one should rephrase the original boundary conditions properly at one single point where the potential and its derivative take a simple analytic form. To achieve this, we use the

fact that the far-field solution of PB equation at a point R^* far away from the colloid surface, i.e., $R^* \gg 1$, can be expressed analytically [36]. Additionally, the following change of variable $\phi \rightarrow \phi - \phi_\infty$ is suitable for simplifying the numerical problem, where ϕ and ϕ_∞ are the electrostatic and well-known Donnan potentials [37], respectively, in units of $ek_B T$, where k_B is the Boltzmann's constant and T the absolute temperature.

Thus, the PB equation and the corresponding boundary conditions can now be written as follows [36],

$$\frac{d^2\phi}{dr^2} + \frac{2}{r} \frac{d\phi}{dr} = -3\eta \frac{Z_{\text{eff}}\lambda_B}{a} - \rho_+(\infty)e^{-\phi} + \rho_-(\infty)e^{\phi}, \quad (3)$$

$$\phi(R^*) = Z_{\text{eff}} \frac{\lambda_B}{a} \left[\frac{\exp(\kappa a)}{1 + \kappa a} \right] \left[\frac{\exp(-\kappa a R^*)}{R^*} \right], \quad (4)$$

$$\phi'(R^*) = -\phi(R^*) \left(\frac{1}{R^*} + \kappa a \right), \quad (5)$$

where $\lambda_B = e^2/\epsilon k_B T$ is the Bjerrum length (in Gaussian units), a is the particle radius, κ is the Debye parameter $\{\kappa^2 = 4\pi\lambda_B [\rho_+(\infty) + \rho_-(\infty)]\}$ and the densities at bulk, which from now on are conveniently written in a dimensionless form, $\rho_\pm(\infty) \rightarrow \rho_\pm(\infty)a^3$, are given by the following relations [36],

$$\rho_+(\infty) = \frac{-3\eta \frac{Z_{\text{eff}}\lambda_B}{a} + \sqrt{\left(3\eta \frac{Z_{\text{eff}}\lambda_B}{a}\right)^2 + (\kappa_{\text{res}}a)^4}}{2}, \quad (6)$$

$$\rho_-(\infty) = \frac{3\eta \frac{Z_{\text{eff}}\lambda_B}{a} + \sqrt{\left(3\eta \frac{Z_{\text{eff}}\lambda_B}{a}\right)^2 + (\kappa_{\text{res}}a)^4}}{2},$$

where $\kappa_{\text{res}}^2 = 8\pi\lambda_B c_s$ is the reservoir screening parameter.

Then, the previous set of equations define the reformulation of the RJ approximation for spherical charged colloids. Basically, we have inverted the original problem, since each point in the new parameters space $(\eta, Z_{\text{eff}}, c_s)$ together with the solution of the previous PB equation provide the corresponding Z_{bare} by simply using the Gauss' law at the colloidal surface, i.e., $\phi'(a) = -Z_{\text{bare}}\lambda_B/a$.

In order to assess the accuracy of our reformulation, we have calculated both the corresponding Debye screening parameter [see Fig. 1(a)] and the effective charge [see Fig. 1(b)] as a function of η for $\kappa_{\text{res}}a = 1$ in the saturation regime, i.e., $Z_{\text{bare}} \rightarrow \infty$. Our results are compared with those obtained by Pianegonda *et al.* [34] and the PB-cell model. Regarding the screening parameter, we observe a good agreement between all renormalization schemes. In particular, it is shown that in this case the salt dominates the screening for $\eta < 0.01$ and therefore κ does not change appreciably; it remains constant. However, for larger volume fractions, i.e., $\eta > 0.01$, the counterions start to dominate and the screening parameter increases notably; this feature has extensively been discussed previously [15]. A similar behavior is observed in the effective charge. Both RJ-like models give basically the same values, although the PB-cell model predicts a dominance of counterions at slightly smaller volume fractions and the effective charge values are always larger than those of the RJ. Additionally, both the main body of Fig. 1(b) and the inset show a particular characteristic predicted within the RJ model which is absent in the PB cell model (the appearance of a minimum whose position depends on the

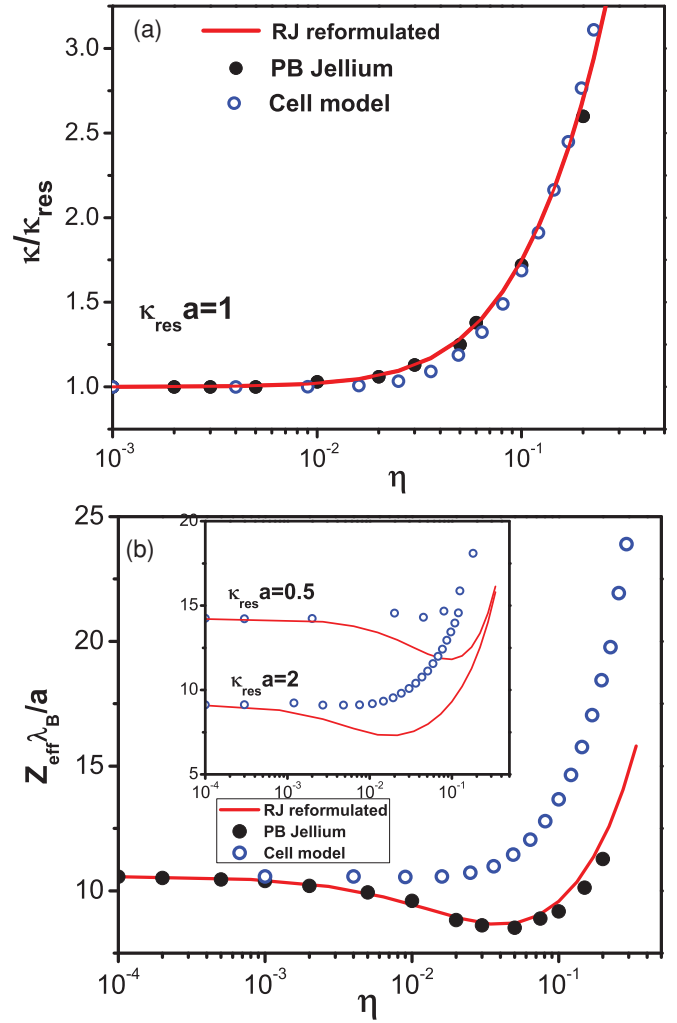


FIG. 1. (Color online) (a) Ratio $\kappa/\kappa_{\text{res}}$ and (b) effective charge, $Z_{\text{eff}}\lambda_B/a$, as a function of η for $\kappa_{\text{res}}a = 1$ in the saturation regime ($Z_{\text{bare}} \rightarrow \infty$) predicted by the RJ model (solid circles), the reformulated one (solid line), and the PB-cell model (open circles). (Inset) The effective charges for different salt conditions, $\kappa_{\text{res}}a = 0.5$ and 2.

salt concentration); such a characteristic has been recently corroborated by scattering experiments [3].

2. Charged rods

Recently, the RJ model has been successfully extended to the case of cylindrical colloids (rods) [34]. In their original work, Pianegonda *et al.* [34] assumed a nematic phase of parallel cylinders with radius a and infinite length b , carrying a bare line charge density ξ_{bare} . In analogy to the RJ for charged spheres, a tagged cylindrical colloid and its cloud of microions possess an effective charge density, ξ_{eff} , forced to coincide with the background charge density, ξ_{back} . In this symmetry the volume fraction is given by $\eta = \pi a^2 \rho$, where ρ is the surface density of colloids in the perpendicular plane to the cylinder axis.

By applying similar ideas, as the ones in the spherical case, the RJ approximation can also be reformulated in the case of charged cylinders demanding self-consistency from the

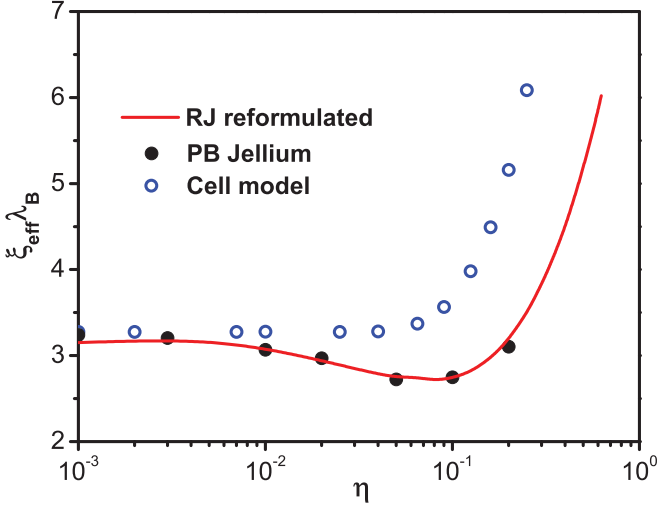


FIG. 2. (Color online) Effective charge density, ξ_{eff} , for charged rods as a function of the volume fraction for $\kappa_{\text{res}}a = 1$ in the saturation regime ($\xi_{\text{bare}} \rightarrow \infty$) predicted by the RJ reformulated (solid line) and the PB-cell model (open symbols). The solid circles are the results from the standard RJ taken from Ref. [27].

beginning, i.e., $\xi_{\text{back}} = \xi_{\text{eff}}$. Thus, the resulting PB equation for charged rods can be rewritten as [36]

$$\frac{d^2\phi}{dr^2} + \frac{1}{r} \frac{d\phi}{dr} = -4\eta\xi_{\text{eff}}\lambda_B - \rho_+(\infty)e^{-\phi} + \rho_-(\infty)e^{\phi}, \quad (7)$$

$$\phi(R^*) = 2\xi_{\text{eff}}\lambda_B \frac{K_0(\kappa a R^*)}{\kappa a K_1(\kappa a)}, \quad (8)$$

$$\phi'(R^*) = \frac{2\xi_{\text{eff}}\lambda_B}{\kappa a K_1(\kappa a)} \frac{\partial K_0(\kappa a R^*)}{\partial R^*}, \quad (9)$$

where K_0 and K_1 are the modified Bessel functions of zeroth and first order, respectively, and the reduced densities at bulk have the same functional form than those given by Eq. (6) but considering the change $3\eta \frac{Z_{\text{eff}}^{a_i}\lambda_B}{a_i} \rightarrow 4\eta\xi_{\text{eff}}\lambda_B$.

To illustrate the accuracy of the reformulation for charged rods, in Fig. 2 we show the behavior of the effective charge density as a function of the volume fraction in the saturation regime ($\xi_{\text{bare}} \rightarrow \infty$) for $\kappa_{\text{res}}a = 1$. Clearly, a similar behavior as in Fig. 1(b) for spherical colloids is observed. Again, at low densities RJ-like models and the cell model give the same results although the PB-cell model predicts slightly larger values when the density increases. The appearance of the minimum is smoother in comparison with the spherical case.

III. POLYDISPERSITY EFFECTS: BINARY MIXTURE CASE

Colloidal suspensions are naturally polydisperse in size and therefore in charge. This intrinsic polydispersity generates a lot of interest due to the large number of features that are not present in a monodisperse suspension. For instance, polydisperse charged colloidal dispersions exhibit a richer structural and phase behavior [38–40].

On the other hand, the concept of charge renormalization has been successfully used for describing the thermodynamics and calculating the structure of monodisperse charged colloidal suspensions, but much less is known about this

phenomenon in the polydisperse case. Recently, Torres *et al.* [17] have extended the PB-cell model to incorporate polydispersity effects; however, within the context of the RJ model they have not been currently studied. Then, for simplicity and to illustrate the extension and applicability of the reformulated RJ approximation, we here discuss results of the charge renormalization in a binary mixture of charged colloids. Therefore, following the previous ideas developed for the monodisperse case, we *a priori* consider self-consistency, i.e., $Z_{\text{back}}^{a_i} = Z_{\text{eff}}^{a_i}$, to avoid the explicit inclusion of the background charge into the PB equation; a_i denotes the particle radius of species i .

Let us consider a system composed of two species of spherical colloids with radius a_1 and a_2 and particle number densities ρ_1 and ρ_2 , respectively. We first consider a system with no added salt, $c_s = 0$. Thus, the PB equation has to be solved for each species separately but taking into account the continuity of the electrostatic potential at the bulk, i.e., the boundary conditions evaluated at distances far away from any particle surface should be the same, and satisfying the electroneutrality condition simultaneously. Then, the PB equation for species i takes the form,

$$\nabla^2\phi_{a_i} = 4\pi\lambda_B(\rho_1 Z_{\text{eff}}^{a_1} + \rho_2 Z_{\text{eff}}^{a_2})(e^{\phi_{a_i}} - 1), \quad (10)$$

with $Z_{\text{eff}}^{a_i}$ as the effective charge of species i . We conveniently express the screening parameter, κ_0 , as

$$\kappa_0^2 = 3 \left(\frac{\eta_{a_1} Z_{\text{eff}}^{a_1}\lambda_B/a_1}{a_1^2} + \frac{\eta_{a_2} Z_{\text{eff}}^{a_2}\lambda_B/a_2}{a_2^2} \right), \quad (11)$$

where the subindex 0 stands for the no-salt case and η_{a_i} is the volume fraction of species i . Additionally, the binary system is fully defined by the total packing fraction, $\eta = \eta_{a_1} + \eta_{a_2}$, and the molar fraction of species i , x_i .

Equation (10) is then solved with the following boundary conditions:

$$\phi_{a_i}(R^*) = Z_{\text{eff}}^{a_i} \frac{\lambda_B}{a_i} \left[\frac{\exp(\kappa_0 a_i)}{1 + \kappa_0 a_i} \right] \left[\frac{\exp(-\kappa_0 R^*)}{R^*} \right], \quad (12)$$

$$\phi'_{a_i}(R^*) = -\phi_{a_i}(R^*) \left(\frac{1}{R^*} + \kappa_0 \right). \quad (13)$$

To numerically solve the above set of equations the effective charge of the other species should remain fixed. Additionally, it is useful to rescale all length quantities with the radius of either particle 1 or 2. Similarly to the monodisperse case, the corresponding bare charge, $Z_{\text{bare}}^{a_i}$, can be easily evaluated via the derivative of the electrostatic potential at the particle surface, $\phi'(a_i)$. This procedure allows us to construct the function $Z_{\text{eff}}^{a_i} = Z_{\text{eff}}^{a_i}(Z_{\text{bare}}^{a_i})$.

Figure 3 shows $Z_{\text{eff}}^{a_1}\lambda_B/a_1$ as a function of $Z_{\text{bare}}^{a_1}\lambda_B/a_1$ in a salt-free binary system with $a_1 = a_2$, $x_1 = 0.5$, and $\eta = 0.1$. Each curve corresponds to a specific value for $Z_{\text{eff}}^{a_2}\lambda_B/a_2$, i.e., we here consider only polydispersity effects in the surface charge of particles of species 2. In general, the behavior is the same as in the monodisperse case [27,36]: The effective charge varies linearly at small bare charges until it reaches a saturation value for large values of the bare one. However, one clearly observes that the value at saturation increases with $Z_{\text{eff}}^{a_2}\lambda_B/a_2$. This mechanism occurs since the electrostatic screening [see Eq. (11)] now makes

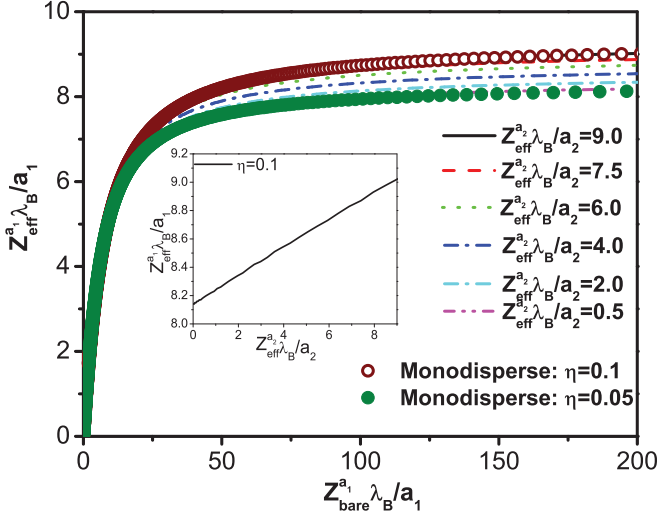


FIG. 3. (Color online) $Z_{\text{eff}}^{a_1} \lambda_B / a_1$ as a function of $Z_{\text{bare}}^{a_1} \lambda_B / a_1$ for a salt-free binary mixture with $x_1 = 0.5$, $a_1 = a_2$, and $\eta = 0.1$. Each curve represents a specific value of $Z_{\text{eff}}^{a_2} \lambda_B / a_2$. Solid and open symbols describe the monodisperse limits $\eta = 0.05$ and $\eta = 0.1$, respectively. (Inset) $Z_{\text{eff}}^{a_1} \lambda_B / a_1$ at saturation ($Z_{\text{bare}}^{a_1} \lambda_B / a_1 \rightarrow \infty$) as a function of $Z_{\text{eff}}^{a_2} \lambda_B / a_2$.

more difficult the condensation of counterions on the particle surface of species 1 and therefore leads to a higher effective charge. Nonetheless, the condensation mechanism becomes more important at lower volume fractions giving rise to a decrease in the effective charge at saturation (data not shown). Additionally, the following limits are observed. For $Z_{\text{eff}}^{a_2} \lambda_B / a_2 \rightarrow 0$, which corresponds to the case of having only charged particles of species 1, $Z_{\text{eff}}^{a_1} \lambda_B / a_1 \rightarrow Z_{\text{eff}}^{a_2} \lambda_B / a_2 \approx 8.14$; this indicates that we recover the monodisperse case for $\eta = 0.05$. On the other hand, for $Z_{\text{eff}}^{a_2} \lambda_B / a_2 = 9$, we obtain the same curve as the one of the monodisperse case when $\eta = 0.1$. As a note, we have considered higher values for $Z_{\text{eff}}^{a_2} \lambda_B / a_2$ and find that the saturation value continues to increase. Interestingly, the inset in Fig. 3 shows that $Z_{\text{eff}}^{a_1} \lambda_B / a_1$ at saturation varies linearly with $Z_{\text{eff}}^{a_2} \lambda_B / a_2$.

The generalization of the above scheme to the case of added salt is straightforward. The PB equation then can be written as

$$\nabla^2 \phi_{a_i} = -\kappa^2 - \rho_+(\infty) e^{-\phi_{a_i}} + \rho_-(\infty) e^{\phi_{a_i}}, \quad (14)$$

where the dimensionless screening parameter reads now as

$$\kappa^4 = \kappa_{\text{res}}^4 + \kappa_0^4, \quad (15)$$

and the local microionic densities at bulk can be simply expressed as a function of both screening parameters,

$$\begin{aligned} \rho_+(\infty) &= \frac{\kappa^2 - \kappa_0^2}{2}, \\ \rho_-(\infty) &= \frac{\kappa_0^2 + \kappa^2}{2}. \end{aligned} \quad (16)$$

Equation (14) then is solved with the boundary conditions given by Eqs. (12) and (13) but replacing κ_0 with κ [Eq. (15)].

We now study the renormalization mechanism in a binary mixture of charged colloids in contact with a salt reservoir. We particularly focus on the effect of the suspension composition by studying simultaneously two different systems with

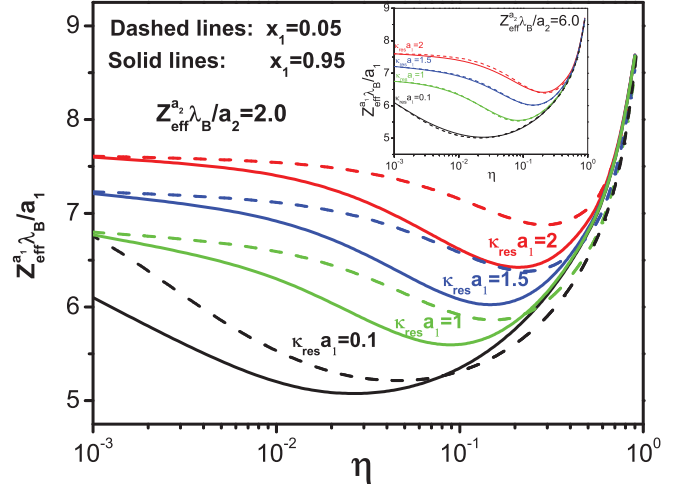


FIG. 4. (Color online) $Z_{\text{eff}}^{a_1} \lambda_B / a_1$ as a function of the volume fraction η for a binary mixture with $Z_{\text{eff}}^{a_2} \lambda_B / a_2 = 2$, $Z_{\text{bare}}^{a_1} \lambda_B / a_1 = 10$, $a_1 = a_2$, $x_1 = 0.05$ (dashed line) [$x_1 = 0.95$ (solid line)]. Each curve represents a specific value of salt concentration, $\kappa_{\text{res}} a_1$. (Inset) $Z_{\text{eff}}^{a_1} \lambda_B / a_1$ as a function of η for the same binary mixture with $Z_{\text{eff}}^{a_2} \lambda_B / a_2 = 6$.

molar fractions $x_1 = 0.05$ and $x_1 = 0.95$, respectively, and $Z_{\text{bare}}^{a_1} \lambda_B / a_1 = 10$. Figure 4 shows $Z_{\text{eff}}^{a_1} \lambda_B / a_1$ for $Z_{\text{eff}}^{a_2} \lambda_B / a_2 = 2$ (main body of caption) and $Z_{\text{eff}}^{a_2} \lambda_B / a_2 = 6$ (inset) as a function of η . In both cases $Z_{\text{eff}}^{a_1} \lambda_B / a_1$ increases with κ_{res} . This is due to the fact that the strong salt contribution to the electrostatic screening makes counterion condensation unfavorable. In addition, similarly to the monodisperse case, the appearance of a minimum whose position depends on the salt concentration is remarkable. This minimum is absent in the polydisperse PB-cell model [17] and, importantly, gives us a qualitative estimation of the boundary at which the counterions start to dominate the electrostatic screening [15]. This can be easily visualized since for $\eta < \eta_m$, with η_m being the volume fraction where the minimum in $Z_{\text{eff}}^{a_1} \lambda_B / a_1$ is found, the effective charge is almost constant (for $\kappa_{\text{res}} a_1 > 0.1$) and the magnitude depends only on the value of κ_{res} , whereas for $\eta > \eta_m$ the effective charge is independent of κ_{res} and the curves collapse onto a single curve, i.e., the monodisperse salt-free curve. Moreover, for $Z_{\text{eff}}^{a_2} \lambda_B / a_2 = 2$ and $x_1 = 0.05$ the effective charge of species 1 is slightly higher than in the case with $x_1 = 0.95$. This means that in the former case, the condensation mechanism of counterions is weaker due to the small amount of colloids of species 1 and the low number of counterions of species 2. However, the inset in Fig. 4 shows that by increasing $Z_{\text{eff}}^{a_2} \lambda_B / a_2$ up to 6, $Z_{\text{eff}}^{a_1} \lambda_B / a_1$ is independent of the composition, but a further increase leads to a higher $Z_{\text{eff}}^{a_1} \lambda_B / a_1$ even in the case where $x_1 = 0.05$ (data not shown).

Figure 5 displays the behavior of $Z_{\text{eff}}^{a_1} \lambda_B / a_1$ as a function of η for two suspensions with molar fractions $x_1 = 0.05$ (dashed line) and $x_1 = 0.95$ (solid line) in the saturation limit of species 1, i.e., $Z_{\text{bare}}^{a_1} \lambda_B / a_1 \rightarrow \infty$, with $Z_{\text{eff}}^{a_2} \lambda_B / a_2 = 9$. Clearly, the trend is basically the same as the one depicted in Fig. 4. Moreover, $Z_{\text{eff}}^{a_1} \lambda_B / a_1$ increases with κ_{res} and the values are higher than those shown previously. It is also noteworthy that the effective charge at saturation for volume fractions below η_m is independent of the composition; however, the counterion

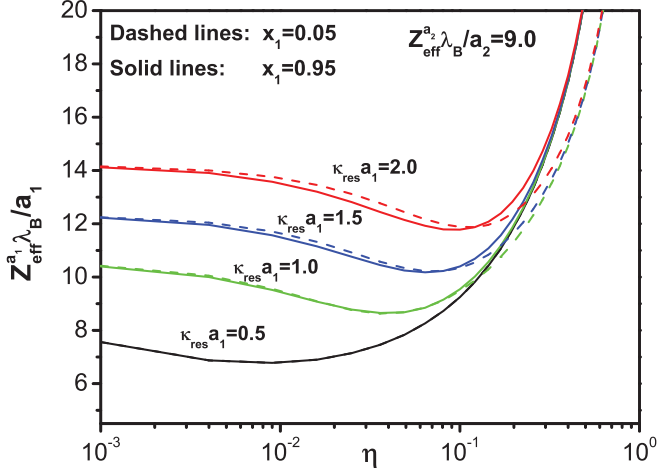


FIG. 5. (Color online) $Z_{\text{eff}}^{a_1} \lambda_B / a_1$ as a function of the volume fraction η for a binary mixture with $Z_{\text{eff}}^{a_2} \lambda_B / a_2 = 9$, $Z_{\text{bare}}^{a_1} \lambda_B / a_1 \rightarrow \infty$, $a_1 = a_2$, $x_1 = 0.05$ (dashed line) [$x_1 = 0.95$ (solid line)]. Each curve represents a specific value of salt concentration, $\kappa_{\text{res}} a_1$.

screening dominance becomes now composition dependent. Both curves clearly collapse in different curves at high volume fractions, i.e., they do not depend on the amount of added salt, but the counterions dominate at smaller volume fractions for the suspension with the higher molar fraction.

We now turn to the case of a salt-free binary mixture made up of large and small particles. Figure 6 depicts $Z_{\text{eff}}^{a_1} \lambda_B / a_1$ as a function of the bare charge in a system with the same molar fraction for each species $x_1 = x_2 = 0.5$, a total volume fraction of $\eta = 0.01$, size ratio $a_1/a_2 = 5$ [Fig. 6(a)] and $a_1/a_2 = 10$ [Fig. 6(b)]. In each figure several values of $Z_{\text{eff}}^{a_2} \lambda_B / a_2$ are considered. We observe in both figures that for small bare charges the linear dependence $Z_{\text{eff}}^{a_1} \approx Z_{\text{bare}}^{a_1}$ is satisfied and at saturation the height of the plateau depends on the effective charge of species 2 and the size ratio. In particular, we note that for small values of $Z_{\text{eff}}^{a_2} \lambda_B / a_2$ the behavior of $Z_{\text{eff}}^{a_1} \lambda_B / a_1$ is almost independent of the size ratio; however, for larger values such dependence becomes clear. In fact, it is evident that the larger size asymmetry, the larger effective charge at saturation. Such an interesting effect can be explained in terms of the screening, which becomes more efficient for a system with an implicit size asymmetry. This is observed directly from Eq. (11), which in units of a_1 takes the following form: $\kappa_0^2 = 3(\eta_{a_1} Z_{\text{eff}}^{a_1} \lambda_B / a_1 + \eta_{a_2} \frac{a_1^2}{a_2^2} Z_{\text{eff}}^{a_2} \lambda_B / a_2)$. Therefore, the second term on the right-hand side of the previous relation, which is proportional to the square of the size ratio, allows us to confirm that a higher size ratio favors the increase of the screening. Thus, the strong screening makes more difficult the counterion condensation on the particle surface of species 1, thus leading to an increase of the effective charge. This interesting mechanism of screening enhancement, obviously not present in the monodisperse case, could be easily used to control the effective charge in mixtures of charged colloids.

So far we have investigated the renormalization mechanisms in a binary mixture of charged colloids through the reformulated RJ model. Particularly, we have shown the importance on the variation of the surface charge, the mixture composition, and the particle size. However, a systematic study

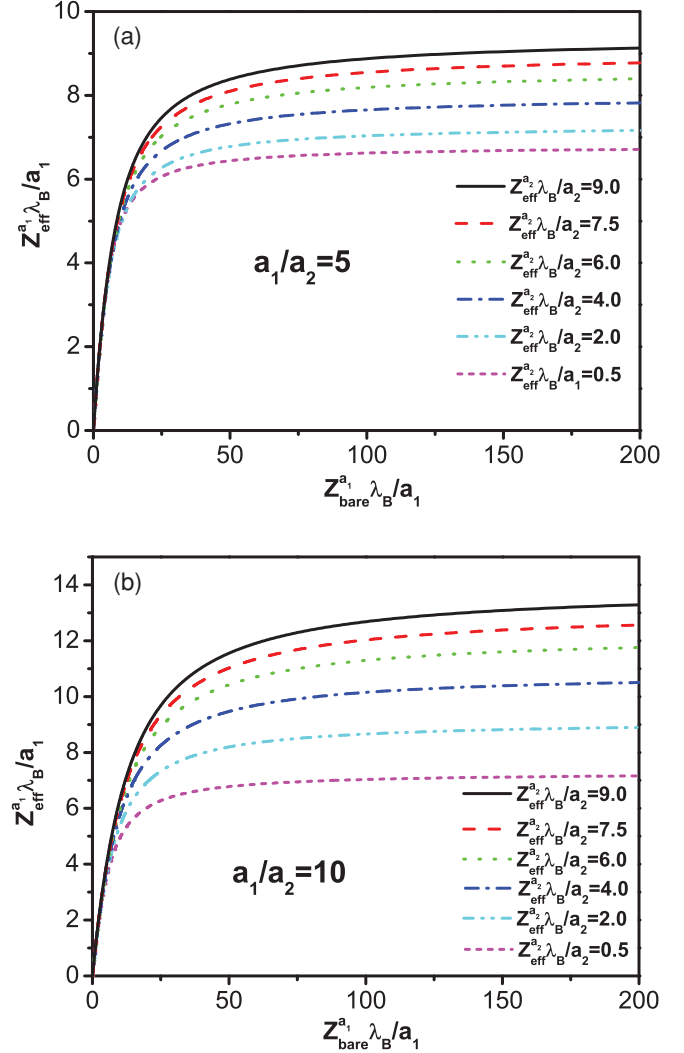


FIG. 6. (Color online) $Z_{\text{eff}}^{a_1} \lambda_B / a_1$ as a function of $Z_{\text{bare}}^{a_1} \lambda_B / a_1$ for a salt-free binary mixture with $x_1 = x_2 = 0.5$, $\eta = 0.01$; size ratio (a) $a_1/a_2 = 5$ and (b) $a_1/a_2 = 10$. Each curve represents a specific value of $Z_{\text{eff}}^{a_2} \lambda_B / a_2$.

on the polydispersity effects in the colloid charge renormalization is still needed to clarify the role of the polydispersity in charged fluids. Furthermore, a full comparison between different mean-field approximations, primitive model calculations, and experiments will allow to determine the accuracy of mean-field models in accounting for both structural and thermodynamic properties of polydisperse charge-stabilized colloidal suspensions [41,42].

IV. CONCLUDING REMARKS

The complete understanding of the (many-body) forces between charged colloids in suspension is far from being clearly understood. However, to reach a better comprehension of the electrostatic interactions among charged objects one has to develop theoretical approaches that allow us to take into account explicitly the main features of the system under study. In particular, during the past few decades, it has been shown that mean-field approximations provide routes for describing both the thermodynamics and effective interactions in

charge-stabilized colloidal suspensions in contact with symmetric salt reservoirs. Moreover, from an experimental point of view, such mean-field models are useful for estimating qualitatively the bare charge of a colloidal particle in an aqueous environment and to calculate the effective potential parameters to be used in the fits of the measured static structure factor.

In this work the RJ mean-field approximation for charged colloids has been employed to understand the mechanisms of charge renormalization in charged colloids in suspension. We found that such an approach, which is known to be useful in describing the thermodynamics of monodisperse suspensions within the fluid phase, can successfully be reformulated by replacing Z_{back} by Z_{eff} directly into the PB equation and rephrasing properly the set of differential equations. Our results were in excellent agreement with the original RJ model. One of the main advantages of the reformulation is that it avoids the use of an iterative protocol to evaluate the effective parameters and it is easy to implement numerically. We also showed that this reformulation can be extended to the cases of nonspherical charged particles (charged rods) and polydisperse charge-stabilized suspensions; the latter case

had not been considered previously. Furthermore, we here obtain interesting results that point toward precise control of the charge renormalization mechanisms by only changing the polydispersity parameters, i.e., surface charge, suspension composition, and particle size distribution. However, the accuracy of our mean-field predictions has to be corroborated using more sophisticated techniques, such as primitive model calculations or experiments. Work along this direction is in progress [42].

Finally, we should remark that we have shown that our reformulation can be easily extended in a large variety of situations and it provides a useful tool to be used for a quick and accurate evaluation of the thermodynamic properties and the effective parameters of charged colloidal suspensions.

ACKNOWLEDGMENTS

Authors thank useful discussions with Gerhard Nägele, Emmanuel Trizac, and Juan Carlos Mixteco-Sánchez. Financial support from PIFI 3.4 and CONACyT (Grants No. 61418/2007 and No. 102339/2008) is acknowledged.

-
- [1] L. Belloni, *J. Phys. Condens. Matt.* **12**, R549 (2000).
 - [2] Y. Levin, *Rep. Prog. Phys.* **65**, 1577 (2002).
 - [3] L. F. Rojas-Ochoa, R. Castañeda Priego, V. Lobaskin, A. Stradner, F. Scheffold, and P. Shurtenberger, *Phys. Rev. Lett.* **100**, 178304 (2008).
 - [4] J. W. Merrill, S. K. Sainis, and E. R. Dufresne, *Phys. Rev. Lett.* **103**, 138301 (2009).
 - [5] P. Linse, *Adv. Polym. Sci.* **185**, 111 (2005).
 - [6] V. Lobaskin and P. Linse, *J. Chem. Phys.* **109**, 3530 (1998).
 - [7] V. Lobaskin and P. Linse, *J. Chem. Phys.* **111**, 4300 (1999).
 - [8] P. Linse and V. Lobaskin, *Phys. Rev. Lett.* **83**, 4208 (1999).
 - [9] V. Lobaskin and P. Linse, *J. Mol. Liq.* **84**, 131 (2000).
 - [10] P. Linse and V. Lobaskin, *J. Chem. Phys.* **112**, 3917 (2000).
 - [11] V. Lobaskin, A. Lyubartsev, and P. Linse, *Phys. Rev. E* **63**, 02041 (2001).
 - [12] V. Lobaskin and K. Qamhieh, *J. Phys. Chem. B* **107**, 8022 (2003).
 - [13] M. Fushiki, *J. Chem. Phys.* **97**, 6700 (1992).
 - [14] J. Dobnikar, D. Halozan, M. Brumen *et al.*, *Comput. Phys. Commun.* **159**, 73 (2004).
 - [15] J. Dobnikar, R. Castañeda-Priego, E. Trizac, and H. H. von Gruenberg, *New J. Phys.* **8**, 277 (2006).
 - [16] L. Belloni, *Coll. Surf. A* **140**, 227 (1998).
 - [17] A. Torres, G. Téllez, and R. van Roij, *J. Chem. Phys.* **128**, 154906 (2008).
 - [18] E. Eggen and R. van Roij, *Phys. Rev. E* **80**, 041402 (2009).
 - [19] A. R. Denton, *J. Phys. Condens. Matter* **20**, 494230 (2008).
 - [20] B. Lu and A. R. Denton, *Comm. Com. Phys.* **7**, 235 (2010).
 - [21] A. R. Denton, *J. Phys. Condens. Matter* **22**, 364108 (2010).
 - [22] M. G. McPhie and G. Nägele, *Phys. Rev. E* **78**, 060401 (2008).
 - [23] P. González-Mozuelos and M. O. de la Cruz, *Physica A* **387**, 5362 (2008).
 - [24] P. González-Mozuelos and M. O. de la Cruz, *Phys. Rev. E* **79**, 031901 (2009).
 - [25] B. L. Arenas-Gómez and P. Gonzalez-Mozuelos, *J. Chem. Phys.* **132**, 014903 (2010).
 - [26] G. I. Guerrero-García, E. González-Tovar, and M. O. de la Cruz, *Soft Matter* **6**, 2056 (2010).
 - [27] E. Trizac and Y. Levin, *Phys. Rev. E* **69**, 031403 (2004).
 - [28] S. Alexander, P. M. Chaikin, P. Grant, G. J. Morales, P. Pincus, and D. Hone, *J. Chem. Phys.* **80**, 5776 (1984).
 - [29] R. Klein, H. H. von Gruenberg, C. Bechinger *et al.*, *J. Phys. Condens. Matter* **14**, 7631 (2002).
 - [30] E. Trizac, L. Bocquet, M. Aubouy, and H. H. von Gruenberg, *Langmuir* **19**, 4027 (2003).
 - [31] B. Beresford-Smith, D. Y. Chan, and D. J. Mitchell, *J. Colloid Interface Sci.* **105**, 216 (1984).
 - [32] R. Castañeda-Priego, L. F. Rojas-Ochoa, V. Lobaskin, and J. C. Mixteco-Sanchez, *Phys. Rev. E* **74**, 051408 (2006).
 - [33] T. E. Colla, Y. Levin, and E. Trizac, *J. Chem. Phys.* **131**, 074115 (2009).
 - [34] S. Pianegonda, E. Trizac, and Y. Levin, *J. Chem. Phys.* **126**, 014702 (2007).
 - [35] T. E. Colla and Y. Levin, *J. Chem. Phys.* **133**, 234105 (2010).
 - [36] J. M. Falcón-González and R. Castañeda Priego, *J. Chem. Phys.* **133**, 216101 (2010).
 - [37] F. G. Donnan, *Chem. Rev.* **1**, 73 (1924).
 - [38] B. D'Aguanno, R. Krause, J. M. Méndez-Alcaraz, and R. Klein, *J. Phys. Condens. Matter* **4**, 3077 (1992).
 - [39] J. M. Méndez-Alcaraz, B. D'Aguanno, and R. Klein, *Langmuir* **8**, 2913 (1992).
 - [40] R. Krause, B. D'Aguanno, J. M. Méndez-Alcaraz, G. Nägele, and R. Klein, *J. Phys. Condens. Matter* **3**, 4459 (1991).
 - [41] Emmanuel Trizac (private communication).
 - [42] J. M. Falcón-González and R. Castañeda-Priego (in preparation).